Néel-State to Valence-Bond-Solid Transition on the Honeycomb Lattice: Evidence for Deconfined Criticality

Sumiran Pujari,[1] Kedar Damle,[2] and Fabien Alet[1]

[1]Laboratoire de Physique Théorique, Université de Toulouse and CNRS, UPS (IRSAMC), F-31062 Toulouse, France
[2]Department of Theoretical Physics, Tata Institute of Fundamental Research, Mumbai 400 005, India
(Received 20 February 2013; revised manuscript received 18 July 2013; published 21 August 2013)

We study a spin-1/2 SU(2) model on the honeycomb lattice with nearest-neighbor antiferromagnetic exchange J that favors Néel order and competing six-spin interactions Q that favor a valence-bond-solid (VBS) state in which the bond energies order at the "columnar" wave vector $\mathbf{K} = (2\pi/3, -2\pi/3)$. We present quantum Monte Carlo evidence for a direct continuous quantum phase transition between Néel and VBS states, with exponents and logarithmic violations of scaling consistent with those at analogous deconfined critical points on the square lattice. Although this strongly suggests a description in terms of deconfined criticality, the measured threefold anisotropy of the phase of the VBS order parameter shows unusual near-marginal behavior at the critical point.

DOI: 10.1103/PhysRevLett.111.087203 PACS numbers: 75.10.Jm, 05.30.Rt, 75.10.Kt

Many interesting materials at low temperature appear to be on the verge of a quantum phase transition involving a qualitative change in the nature of the ground state [1]. When one of the two competing $T = 0$ phases spontaneously breaks a symmetry, the transition can be studied using a path integral representation with a Landau-Ginzburg action [2] written in terms of the order parameter that characterizes the broken symmetry phase [1]. If phases on two sides of the critical point break different symmetries, Landau-Ginzburg theory generically predicts a direct first-order transition or a two-step transition with an intermediate phase. However, this path integral description in terms of order-parameter variables can sometimes involve Berry phases in a nontrivial way [3–5]. The presence of Berry phases, which correspond to complex Boltzmann weights for the corresponding classical statistical mechanics problem in one higher dimension [1], can invalidate the conclusions reached by the Landau-Ginzburg approach.

In some of these cases, it is useful [6] to think in terms of topological defects in one of the ordered states and view the competing ordered state as being the result of the condensation of these topological defects—this description [6] makes sense only if the quantum numbers carried by defects in one phase match those of the order-parameter variable in the other phase. Under certain conditions, this alternate "non-Landau" description generically predicts a direct continuous transition [7,8] between the two ordered states, in contrast to predictions of classical Landau-Ginzburg theory. Square lattice $S = 1/2$ antiferromagnets undergoing a transition from a ground state with nonzero Néel order parameter $\vec{M}_s$ to a valence-bond-solid (VBS) ordered state, in which the "bond energies" (singlet projectors) $P_{\langle ij\rangle} \equiv 1/4 - \vec{S}_i \cdot \vec{S}_j$ on nearest-neighbor bonds $\langle ij\rangle$ in the $\hat{x}$ ($\hat{y}$) direction develop long-range order at the "columnar wave vectors" $\mathbf{K}_1 = (\pi, 0)$ [$\mathbf{K}_2 = (0, \pi)$], provide the best-studied example of such "deconfined critical points" [7,8]. In this case, Z_4 vortices in the complex VBS order parameter Ψ carry a net spin $S = 1/2$ in their core, suggesting that the onset of Néel order can be studied using a CP^1 description of $\vec{M}_s$: $\vec{M}_s = z^*_\alpha \vec{\sigma}_{\alpha\beta} z_\beta$, where $\vec{\sigma}$ are Pauli matrices and the Z_4 vortices are represented by a two-component complex bosonic field z_α coupled to a compact U(1) gauge field $\mathcal{A}_\mu$ [6–8], whose space-time monopoles correspond [4,9] to hedgehog defects in the Néel order. Only quadrupled hedgehog defects (corresponding to fourfold anisotropy in the phase of Ψ) survive the destructive interference of Berry phases on the square lattice [3–5,9], and their irrelevance at criticality [7,8] leads to a noncompact (monopole-free [10–12]) CP^1 (NCCP^1) description of this transition.

Here, we use quantum Monte Carlo (QMC) simulations [13–15] to study a spin-1/2 Heisenberg model on the honeycomb lattice with nearest-neighbor antiferromagnetic exchange J that favors Néel order and competing six-spin interactions Q that favor VBS order at the "columnar wave vector" $\mathbf{K} = (2\pi/3, -2\pi/3)$

$$H = -J\sum_{\langle ij\rangle} P_{\langle ij\rangle} - Q \sum_{\langle\langle ijklmn\rangle\rangle} (P_{\langle ij\rangle}P_{\langle kl\rangle}P_{\langle mn\rangle} + P_{\langle jk\rangle}P_{\langle lm\rangle}P_{\langle ni\rangle}),$$

where $\langle\langle ijklmn\rangle\rangle$ denotes hexagonal plaquettes (Fig. 1). We find evidence for a direct continuous Néel-VBS transition at $(Q/J)_c \equiv q_c \approx 1.190(6)$, with correlation length exponent $\nu \approx 0.54(5)$ and anomalous exponents $\eta_{\text{Néel}} \approx 0.30(5)$ and $\eta_{\text{VBS}} \approx 0.28(8)$; within errors, these values match corresponding results at the Néel-columnar VBS transition on the square lattice [16–18]. In addition, we find evidence for apparently logarithmic violations of finite-temperature scaling of the uniform spin susceptibility χ_u and stiffness ρ_s, analogous to the square-lattice case [17]. However, in sharp contrast to the square-lattice transition at which the *fourfold* anisotropy vanishes for large systems [18–20], a careful study of the *threefold* anisotropy

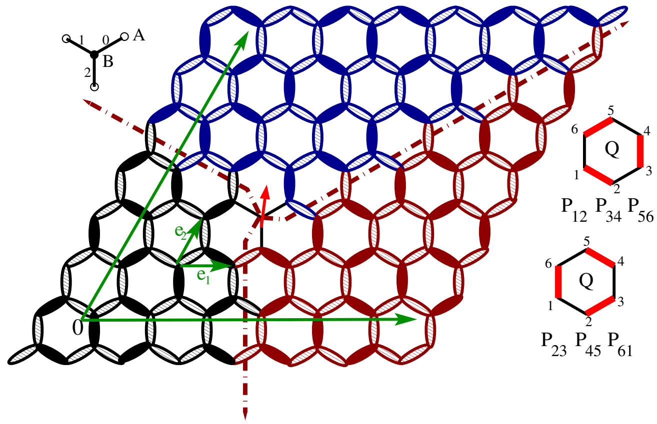

FIG. 1 (color online). The honeycomb lattice has a two-site basis (labeled A and B) and elementary Bravais lattice translations $\hat{e}_1$ and $\hat{e}_2$, with distances from origin specified in units of $\hat{e}_1$ and $\hat{e}_2$. Three types of bonds (labeled 0, 1, 2), oriented along the three principal directions, "belong" to each Bravais lattice site. Columnar and plaquette VBS order at wave vector **K** correspond to different choices of the order-parameter phase, with solid filled dimers on a link $\langle ij \rangle$ denoting high (low) values of $\langle P_{\langle ij \rangle} \rangle$ in the columnar (plaquette) state. Here, three domain walls meet at the core of the Z_3 vortex, which carries a net $S = 1/2$ spin. Also shown is a depiction of the six-spin interaction terms in H.

in the phase of Ψ reveals surprising near-marginal behavior on the honeycomb lattice.

To put these results in context, we first note that Z_3 vortices in Ψ carry a net spin $S = 1/2$ in their core on the honeycomb lattice (Fig. 1) analogous to Z_4 vortices on the square lattice. Therefore, a continuum CP^1 description [6] is again appropriate. The monopole creation operator in the CP^1 description transforms under lattice symmetries in *the same way* as the complex VBS order parameter Ψ at the "columnar wave vectors" on both the honeycomb and square lattices, allowing one to view these VBS states as monopole condensates [4,5,7,8]. On the honeycomb lattice, it picks up a $2\pi/3$ phase under lattice rotations. Therefore, insertions of *tripled* monopoles are allowed on the honeycomb lattice and manifest themselves as a *threefold* anisotropy felt by the phase of Ψ. If this is relevant, one expects the correct long-wavelength description of the transition to be a conventional Landau-Ginzburg theory written in terms of $\vec{M}_s$ and Ψ and the transition to be first order in the simplest scenario or proceed in two steps with an intermediate phase [7,8]. On the square lattice, only quadrupled monopoles are allowed in the CP^1 description since Ψ picks up a $\pi/2$ phase under rotations. These can be straightforwardly argued [7,8] to be irrelevant in the NCCP^{N-1} theory at $N = 2$ by noting that they are irrelevant both at $N = 1$ [5,7,21–23] and in the $N \to \infty$ limit [5,7,21], leading to a NCCP^1 description of the transition.

Thus, on one hand, the continuous nature and measured exponents of the honeycomb lattice transition as well as the finite-temperature behavior of ρ_s and χ_u point to a NCCP^1 description and suggest that tripled monopoles are irrelevant at the NCCP^1 fixed point, allowing the physics of deconfined criticality to control universal properties of transitions to VBS order at wave vector **K**. If the transition to plaquette VBS order at the same wave vector **K** (Fig. 1) in the frustrated J_1-J_2 is indeed direct and continuous [24–27], our results suggest, on grounds of universality, that it too would be governed by the NCCP^1 fixed point. On the other hand, our observation of near-marginal behavior of the three-fold anisotropy at criticality suggests that threefold monopoles remain important ingredients of the honeycomb lattice transition at large scales, making it remarkable that other signatures of the transition conform to what one expects at the NCCP^1 critical point. The physical $N = 2$ case lies between two contrasting extremes of the NCCP^{N-1} theory: tripled monopoles are relevant at $N = 1$ [5,7,21,22] and lead to a weakly first-order transition [28], but strongly irrelevant in the $N \to \infty$ limit [5,7,21]. Our results therefore suggest that tripled monopoles switch from relevant to irrelevant behavior at or very close to $N = 2$ as one increases N in the NCCP^{N-1} theory.

It is quite clear that the continuous transition studied here is very different from transitions to staggered VBS order on square and honeycomb lattices [29,30], whose strongly first-order nature can be attributed [30] to the spinless cores of vortices in staggered VBS states [6]. Indeed, most of our results on universal critical properties are very similar to previous QMC simulations of computationally tractable spin models exhibiting Néel-columnar VBS transitions on the square lattice [16–18,20,31–37]. Whereas some of these studies [16–18,20,31–35] have interpreted these square-lattice results within the framework of the NCCP^1 theory, albeit with some logarithmic violations of scaling [17,31–33], other studies [36,37] have interpreted very similar numerical data in terms of a flow to a very weakly first-order transition at large length scales—this is motivated by data on lattice-discretized NCCP^1 models [38,39], some of which exhibit first-order behavior [39]. Our work adds another dimension to this debate by demonstrating that results otherwise consistent with the NCCP^1 description are accompanied by significant anisotropy in the phase of Ψ at the honeycomb lattice transition.

We study H on $L \times L$ honeycomb lattices (Fig. 1) of $2L^2$ spins, with periodic boundary conditions and L a multiple of 12 up to $L = 72$. We use a $T = 0$ projector QMC algorithm [14], with a sufficiently large projection length cL^3 (c ranging from 4 to 12) to ensure convergence to the ground state. At small q values, the ground state is Néel ordered, as characterized by the Néel order parameter $\vec{M}_s = \sum_{\vec{r}} \vec{m}(\vec{r})/(2L^2)$, where $\vec{m}$ is the local Néel field $\vec{m}(\vec{r}) = \vec{S}_{\vec{r}A} - \vec{S}_{\vec{r}B}$. Here, $\vec{r}A$ ($\vec{r}B$) refers to the A (B) sublattice site belonging to Bravais lattice site $\vec{r}$ (Fig. 1). To locate the quantum phase transition where Néel order is lost, we compute the "dimensionless" Binder cumulant

$g_{\vec{M}_s} = \langle (\vec{M}_s^2)^2 \rangle / \langle \vec{M}_s^2 \rangle^2$. It is expected to obey a scaling form $F_{g_{\vec{M}_s}}(\Delta q_N)$ if there is a continuous transition at q_{cN}. Here, $F_{g_{\vec{M}_s}}$ is a universal scaling function of the argument $\Delta q_N \equiv (q - q_{cN}) L^{1/\nu_N}$ where ν_N is the correlation length exponent associated with Néel correlations. In the vicinity of such a transition, we also expect the scaling form $\langle \vec{M}_s^2 \rangle = L^{-(1+\eta_{\text{Néel}})} G_{\vec{M}_s}(\Delta q_N)$ for the corresponding dimensionful quantity.

At large q, we find that VBS order develops at the "columnar wave vector" $\mathbf{K}$. This is characterized by the VBS order parameter $\Psi = \sum_{\vec{r}} V_{\vec{r}} / (2L^2)$, where $V_{\vec{r}}$ is the local VBS order-parameter field

$$V_{\vec{r}} = (P_{\vec{r}0} + e^{2\pi i/3} P_{\vec{r}1} + e^{4\pi i/3} P_{\vec{r}2}) e^{i\mathbf{K}\cdot\vec{r}}.$$

Here, $P_{\vec{r}\mu}$ ($\mu = 0, 1, 2$) denotes the singlet projector on the bond μ "belonging" to Bravais lattice site $\vec{r}$ (Fig. 1). To quantify the strength of VBS order, we compute $\langle |\Psi|^2 \rangle = \langle \Psi^\dagger \Psi \rangle$. The phase of Ψ distinguishes between two kinds (columnar vs plaquette) of threefold symmetry breaking VBS order at wave vector $\mathbf{K}$. In the $T = 0$ QMC simulations, information on this phase is obtained from the estimator E_Ψ, whose average $\overline{E_\Psi}$ over the QMC run gives the quantum-mechanical expectation value $\langle \Psi \rangle$. Although E_Ψ is a basis-dependent quantity, the histogram of its phase can nevertheless be used to distinguish between the different VBS states at the same wave vector [18,20]. The VBS transition can be located by focusing again on a dimensionless quantity, the (basis-dependent) Binder cumulant [40] of E_Ψ defined as $g_{E_\Psi} \equiv \overline{|E_\Psi|^4} / (\overline{|E_\Psi|^2})^2$, which is again expected to obey a scaling form $F_{g_{E_\Psi},D}(\Delta q_D)$ if VBS order is lost via a continuous $T = 0$ transition at q_{cD}. The argument $\Delta q_D \equiv (q - q_{cD}) L^{1/\nu_D}$ of the universal scaling function $F_{g_{E_\Psi},D}$ uses ν_D, the correlation length exponent associated with VBS correlations. Close to such a continuous transition, we also expect the corresponding scaling form $\langle |\Psi|^2 \rangle = L^{-(1+\eta_{\text{VBS}})} G_\Psi(\Delta q_D)$ for the dimensionful observable.

We pinpoint the $T = 0$ Néel and VBS transitions from the crossings of the Binder ratios $g_{\vec{M}_s}$ and g_{E_Ψ} as a function of q for various L values—at this stage, we do not assume that the two transitions coincide. Given the relatively sharp nature of the crossings and the monotonic nature of their q dependence for fixed L values (Fig. 2), we are confident that the transition(s) is (are) continuous. We fit data for each dimensionless ($g_{\vec{M}_s}$, g_{E_Ψ}) and (appropriately scaled) dimensionful quantity $\langle \vec{M}_s^2 \rangle L^{1+\eta_{\text{Néel}}}$, $\langle |\Psi|^2 \rangle L^{1+\eta_{\text{VBS}}}$, in the critical range to a polynomial function of $(q - q_c) L^{1/\nu}$ (corresponding to a polynomial approximation of scaling functions), with the corresponding q_c, ν, η and polynomial coefficients being fitting parameters. For each dimensionless quantity, the best-fit values vary somewhat depending on the range of L and q studied. Results of such fits for one choice of data set for the dimensionless quantities are displayed as lines in Fig. 2, with the corresponding scaling collapse displayed in Fig. 3. Similar results for Néel and VBS correlators [41] confirm this.

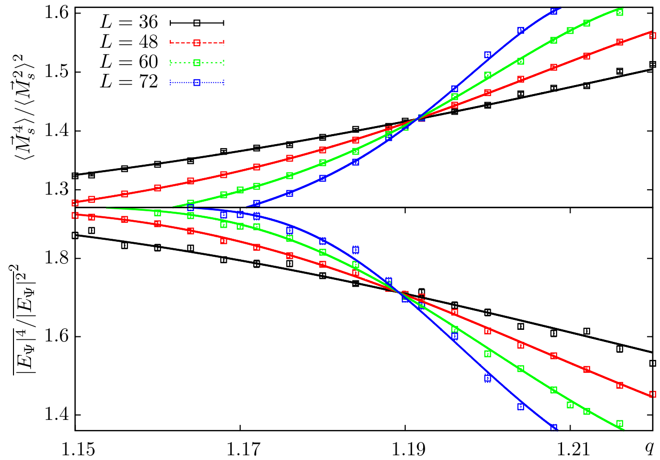

FIG. 2 (color online). Binder cumulants of $\vec{M}_s$ and E_Ψ as a function of q for different sizes L (symbols), fit to a polynomial in $(q - q_{cD/N}) L^{1/\nu_{D/N}}$ (lines) with best-fit values $\nu_N = 0.5080$, $\nu_D = 0.5237$, $q_{cN} = 1.1912$, and $q_{cD} = 1.1892$. Best-fit values are for the $L \geq 48$ part of the displayed data.

On the basis of a detailed study of such fits, we estimate $q_{cN} \approx 1.1936(24)$, $q_{cD} \approx 1.1864(28)$, $\nu_N = 0.51(3)$, $\nu_D = 0.55(4)$, $\eta_{\text{Néel}} = 0.30(5)$, and $\eta_{\text{VBS}} = 0.28(8)$. The error bars quoted here reflect not just the error in determining best-fit values for a given data set for each quantity and variation in these best-fit values from quantity to quantity but also the dependence of these best-fit values on the

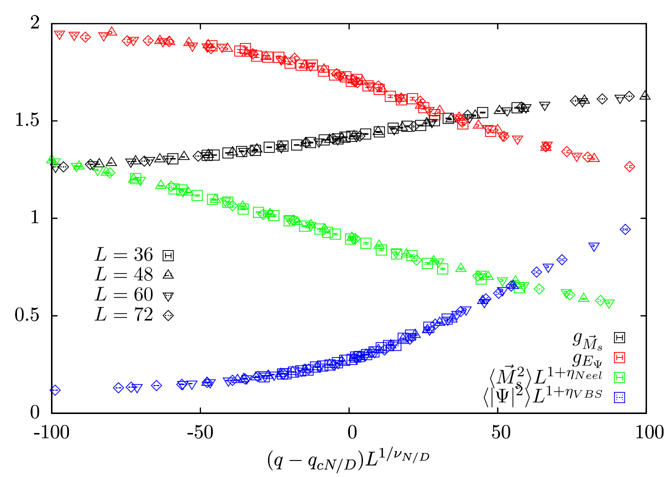

FIG. 3 (color online). Scaling collapse of Binder cumulants of $\vec{M}_s$ and E_Ψ, using values of q_{cD}, q_{cN}, ν_D, and ν_N quoted in legend of Fig. 2. Similar collapses for $\langle \vec{M}_s^2 \rangle L^{1+\eta_{\text{Néel}}}$, $\langle |\Psi|^2 \rangle L^{1+\eta_{\text{VBS}}}$ are also displayed, obtained using the following best-fit values: $q_{cN} = 1.1956$, $\nu_N = 0.5003$, $\eta_{\text{Néel}} = 0.3539$ ($\langle \vec{M}_s^2 \rangle$), $q_{cD} = 1.1864$, $\nu_D = 0.558$, and $\eta_{\text{VBS}} = 0.25$ ($\langle |\Psi|^2 \rangle$). Best-fit values are for the $L \geq 48$ part of the displayed data.

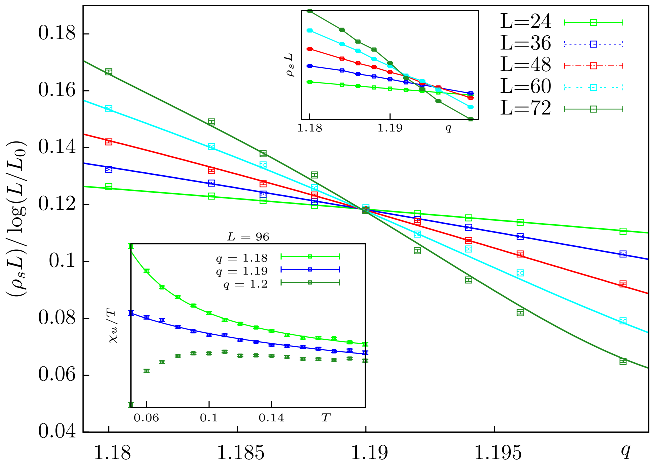

FIG. 4 (color online). $\rho_s L$ does not obey standard quantum-critical scaling $\rho_s L = h((q - q_{cN})L^{1/\nu_N})$ with dynamical exponent $z = 1$ (for instance, see drift in $\beta = 2L$ data shown in top inset). In contrast $\rho_s L/\log(L/L_0)$ with $L_0 = 0.37$ shows excellent scaling. Symbols are QMC data, and lines are best fit to this modified scaling form, with $q_{cN} \approx 1.190(2)$ and $\nu_N \approx 0.54(2)$ in agreement with our $T = 0$ results. Bottom inset: Temperature dependence of χ_u/T close to criticality. In the Néel phase ($q = 1.18$), QMC data (symbols) are well fit by $\chi_u/T = a + b/T$, whereas on the VBS side ($q = 1.2$), a sharp drop is observed as expected. Close to criticality ($q = 1.19$), QMC data are better fit by $\chi_u/T = c + d\log(J/T)$. Lines are fits to the above forms with $a = 0.024$, $b = 0.0005$, $c = 0.022$, and $d = 0.0024$.

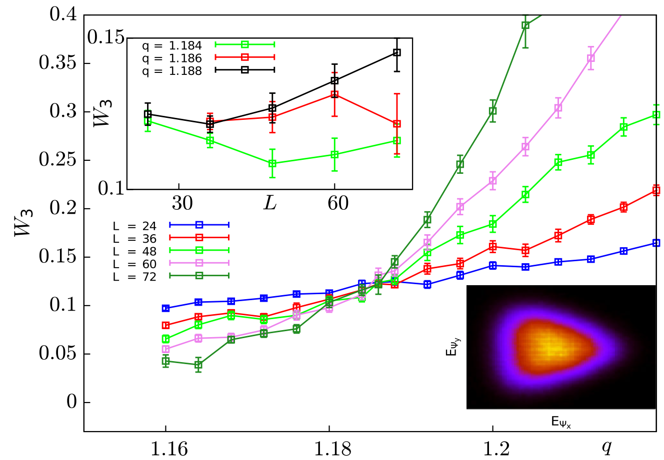

FIG. 5 (color online). The dimensionless Z_3-anisotropy parameter W_3 scales to zero with increasing L value in the Néel phase but grows with size in the columnar VBS phase. Top inset zooms in on the behavior of near-critical systems, which display nearly scale-independent behavior. Bottom inset: histogram of E_Ψ for $L = 36$ at $q = 1.184$ close to q_{cD}. The brightness of each color patch reflects the weight.

data set used, i.e., the size of the critical window in q and the range of L values used in the fits. We also emphasize that our estimates of $\eta_{\rm VBS}$ and $\eta_{\rm Néel}$ depend sensitively on the value of q_c, resulting in the relatively large error bars quoted here. Nevertheless, we are in a position to exclude the relatively tiny values of η that characterize conventional second-order critical points in $2 + 1$ dimensions. Since ν_N *coincides* with ν_D within error bars, and the allowed ranges of q_{cN} and q_{cD} almost touch at the 1σ level, the simplest interpretation of our data is that Néel order is lost and VBS order sets in at a single continuous $T = 0$ transition whose location is estimated to be $q_c \approx 1.190(6)$, with correlation exponent $\nu = 0.54(5)$ and anomalous exponents $\eta_{\rm Néel} = 0.30(5)$ and $\eta_{\rm VBS} = 0.28(8)$. This, taken together with the relatively large values of $\eta_{\rm Néel}$ and $\eta_{\rm VBS}$ characteristic of deconfined critical points, suggests an interpretation in terms of deconfined criticality.

Indeed, our estimates of $\eta_{\rm VBS}$, $\eta_{\rm Néel}$, and ν as well as of the universal critical value $g^* = 1.42(1)$ of the Néel Binder ratio at the $T = 0$ transition are consistent within errors with values for the analogous transition on the square lattice [16–18]. We also study the temperature dependence of the uniform spin susceptibility χ_u and the antiferromagnetic spin stiffness ρ_s using finite-T QMC methods [15] at low temperatures in the vicinity of this $T = 0$ transition. As is clear from Fig. 4, data for these quantities do not fit well to standard scaling predictions. However, excellent data collapse is obtained upon inclusion of logarithmic violations of scaling, using the same functional forms employed earlier on the square lattice [17]. These logarithmic violations may be related to (near) marginal operators in the NCCP^1 theory itself [42,43].

Finally, we turn to a study of the effective threefold anisotropy felt by the phase of Ψ at criticality, as seen in histograms of E_Ψ near q_c. The phase θ of E_Ψ (inset of Fig. 5) appears to feel significant anisotropy near the $T = 0$ transition on the honeycomb lattice. To quantify this anisotropy in the distribution $P(E_\Psi)$ near the critical point, we use a (dimensionless) estimator $W_3 = \int dE_\Psi P(E_\Psi) \times \cos(3\theta)$, designed to be 0 for a U(1)-symmetric distribution and 1 (-1) for ideal columnar (plaquette) VBS states (Fig. 1). In Fig. 5, we see that W_3 appears to saturate to a scale-independent constant at large L as the transition is approached from the Néel phase, before growing with size as one moves into a columnar VBS state. This near-marginal behavior of the anisotropy in $P(E_\Psi)$ at the largest scales accessible to our simulations is *very* different from the U(1) symmetric probability distribution of E_Ψ seen near the square-lattice critical point [18,19]. A more refined scaling analysis [41] yields the same result, leading us to our earlier suggestion that threefold monopole insertions are (very close to) marginal at the NCCP^1 critical point—this is consistent with recent parallel work that discusses the relevance of q-fold monopoles in SU(N) spin models [44,45].

We thank A. Banerjee, L. Balents, S. Capponi, R. Kaul, A. Läuchli, M. Mambrini, A. Paramekanti, and P. Pujol for useful discussions and D. Dhar and S. N. Majumdar for a critical reading of a previous version of our manuscript. We acknowledge computational resources from TIFR

Mumbai, GENCI-CCRT (Grant No. 2012050225), and CALMIP. This research is supported by the Indo-French Centre for the Promotion of Advanced Research (IFCPAR/CEFIPRA) under Project 4504-1, French ANR program Grant No. ANR-08-JCJC-0056-01, and in part by the National Science Foundation under Grant No. NSF PHY11-25915, during a visit by one of us (K. D.) to KITP, Santa Barbara. We also acknowledge support for collaborative visits from the University Paul Sabatier, Toulouse (K. D.) and TIFR (S. P.).

[1] S. Sachdev and B. Keimer, Phys. Today **64**, No. 2, 29 (2011).
[2] L. D. Landau, E. M. Lifshitz, and E. M. Pitaevskii, *Statistical Physics* (Butterworth-Heinemann, New York, 1999).
[3] F. D. M. Haldane, Phys. Rev. Lett. **61**, 1029 (1988).
[4] N. Read and S. Sachdev, Phys. Rev. Lett. **62**, 1694 (1989).
[5] N. Read and S. Sachdev, Phys. Rev. B **42**, 4568 (1990).
[6] M. Levin and T. Senthil, Phys. Rev. B **70**, 220403 (2004).
[7] T. Senthil, L. Balents, S. Sachdev, A. Vishwanath, and M. P. A. Fisher, Phys. Rev. B **70**, 144407 (2004).
[8] T. Senthil, A. Vishwanath, L. Balents, S. Sachdev, and M. P. A. Fisher, Science **303**, 1490 (2004).
[9] A. D'Adda, P. Di Vecchia, and M. Luscher, Nucl. Phys. **B146**, 63 (1978); E. Witten, Nucl. Phys. **B149**, 285 (1979); S. Coleman, Ann. Phys. (N.Y.) **101**, 239 (1976).
[10] M.-h. Lau and C. Dasgupta, J. Phys. A **21**, L51 (1988); Phys. Rev. B **39**, 7212 (1989).
[11] M. Kamal and G. Murthy, Phys. Rev. Lett. **71**, 1911 (1993).
[12] O. I. Motrunich and A. Vishwanath, Phys. Rev. B **70**, 075104 (2004).
[13] A. W. Sandvik, Phys. Rev. Lett. **95**, 207203 (2005).
[14] A. W. Sandvik and H. G. Evertz, Phys. Rev. B **82**, 024407 (2010).
[15] O. F. Syljuåsen and A. W. Sandvik, Phys. Rev. E **66**, 046701 (2002).
[16] A. W. Sandvik, Phys. Rev. B **85**, 134407 (2012).
[17] A. W. Sandvik, Phys. Rev. Lett. **104**, 177201 (2010).
[18] A. W. Sandvik, Phys. Rev. Lett. **98**, 227202 (2007).
[19] J. Lou and A. W. Sandvik, Phys. Rev. B **80**, 212406 (2009).
[20] J. Lou, A. W. Sandvik, and N. Kawashima, Phys. Rev. B **80**, 180414 (2009)
[21] S. Sachdev and R. A. Jalabert, Mod. Phys. Lett. B **04**, 1043 (1990).
[22] M. Oshikawa, Phys. Rev. B **61**, 3430 (2000).
[23] J. Lou, A. W. Sandvik, and L. Balents, Phys. Rev. Lett. **99**, 207203 (2007).
[24] A. F. Albuquerque, D. Schwandt, B. Hetényi, S. Capponi, M. Mambrini, and A. M. Läuchli, Phys. Rev. B **84**, 024406 (2011).
[25] Z. Zhu, D. A. Huse, and S. R. White, Phys. Rev. Lett. **110**, 127205 (2013).
[26] R. Ganesh, J. van den Brink, and S. Nishimoto, Phys. Rev. Lett. **110**, 127203 (2013).
[27] S.-S. Gong, D. N. Sheng, O. I. Motrunich, and M. P. A. Fisher, arXiv:1306.6067.
[28] W. Janke and R. Villanova, Nucl. Phys. **B489**, 679 (1997).
[29] A. Sen and A. W. Sandvik, Phys. Rev. B **82**, 174428 (2010).
[30] A. Banerjee, K. Damle, and A. Paramekanti, Phys. Rev. B **83**, 134419 (2011).
[31] A. Banerjee, K. Damle, and F. Alet, Phys. Rev. B **82**, 155139 (2010).
[32] A. Banerjee, K. Damle, and F. Alet, Phys. Rev. B **83**, 235111 (2011).
[33] R. K. Kaul, Phys. Rev. B **84**, 054407 (2011).
[34] R. K. Kaul and A. W. Sandvik, Phys. Rev. Lett. **108**, 137201 (2012).
[35] R. G. Melko and R. K. Kaul, Phys. Rev. Lett. **100**, 017203 (2008).
[36] F. J. Jiang, M. Nyfeler, S. Chandrasekharan, and U. J. Wiese, J. Stat. Mech.: Theory Exp. (2008), P02009.
[37] K. Chen, Y. Huang, Y. Deng, A. B. Kuklov, N. V. Prokof'ev, and B. V. Svistunov, Phys. Rev. Lett. **110**, 185701 (2013).
[38] O. I. Motrunich and A. Vishwanath, arXiv:0805.1494.
[39] A. B. Kuklov, M. Matsumoto, N. V. Prokof'ev, B. V. Svistunov, and M. Troyer, Phys. Rev. Lett. **101**, 050405 (2008).
[40] We use g_{E_Ψ} instead of the Binder cumulant $\langle|\Psi|^4\rangle/\langle|\Psi|^2\rangle^2$ due to technical difficulties in measuring $\langle|\Psi|^4\rangle$.
[41] See the Supplemental Material at http://link.aps.org/supplemental/10.1103/PhysRevLett.111.087203 for details on scaling analysis of the Néel and VBS correlators as well as Z_3 anisotropy.
[42] F. S. Nogueira and A. Sudbo, Phys. Rev. B **86**, 045121 (2012).
[43] L. Bartosch, arXiv:1307.3276.
[44] M. S. Block, R. G. Melko, and R. K. Kaul, arXiv:1307.0519.
[45] K. Harada, T. Suzuki, T. Okubo, H. Matsuo, J. Lou, H. Watanabe, S. Todo, and N. Kawashima, arXiv:1307.0501.